Chapter Seven:

NLRX1 regulates TNF-α-induced mitochondria-lysosomal crosstalk to maintain the tumorigenic potential of breast cancer cells

An increased level of proinflammatory cytokines, including TNF-α in TME regulates the bioenergetic capacity, immune evasion and survival of cancer cells. We published the results discussed in Chapter Two which further strengthens the concepts that mitochondrial immune signaling proteins including NLRX1 modulates mitochondrial bioenergetic capacity, in addition to the regulation of innate immune response (Singh et al., 2018). As discussed in Chapter One and Chapter Two, NLRX1 expression is differentially regulated in multiple human cancer subtypes suggesting a complex role of NLRX1-regulated mitochondrial function in controlling the tumorigenicity of cancer cells. Recent reports suggested that an optimal oxidative phosphorylation (OxPhos) capacity is required for the maintenance of functional lysosomes and autophagy flux during adaptive immune response and inflammation (Baixauli et al., 2015; Demers-Lamarche et al., 2016). The role of NLRX1 in regulation of mitochondrial and lysosomal function to modulate autophagy flux during inflammatory conditions is largely unknown. In the present study, we investigated role of NLRX1 in modulating TNF-α induced autophagy flux, mitochondrial turnover and its implication in regulating tumorigenic potential of breast cancer cells.

7.1 NLRX1 expression is upregulated in invasive breast cancer cell lines and metastatic tumors

To investigate the association of NLRX1 expression levels with the invasive phenotype of breast tumors, we analyzed its expression in different breast cancer cell lines. The relative expression of NLRX1 in four ER/PR positive cells (MCF-7, ZR-75-1, BT-474 and T47D) and two ER/PR negative cells (MDA-MB-231 and HBL100) was analyzed by quantitative PCR (Fig. 7.1A). NLRX1 expression levels were significantly high in MDA-MB-231 and HBL100 than ER/PR positive cells. Similarly, the analysis of protein levels in same set of cell lines indicated a strong expression of NLRX1 in MDA-MB-231 and HBL100 cells as compared to ER/PR positive cells (Fig. 7.1B).

The expression level of NLRX1 were further analyzed in tumor tissues obtained from breast cancer patients. Immunoblot analysis revealed that NLRX1 levels were upregulated in all ER/PR negative tumors while downregulated in ER/PR positive breast tumors (Fig. 7.1C). Similarly, the mRNA levels of NLRX1 were six-fold high in all ER/PR nega-

tive tumors as compared to non- tumorous adjacent tissue (NAT) (Fig. 7.1D). The expression of NLRX1 was also analyzed by immunohistochemistry (Fig. 7.1E). An intense staining of NLRX1 was observed in tumor tissue as compared to NAT. Finally, meta-analysis of mRNA expression profiles of invasive breast carcinoma available in publicly accessible databases displayed a strong association of upregulatedNLRX1 expression levels with ER/PR negativity and advanced stage tumors (Fig. 7.1F, G and H). These evidences suggested that NLRX1 is expressed at higher levels in invasive breast cancer cell lines and metastatic tumors and display an inverse correlation with ER/PR status.
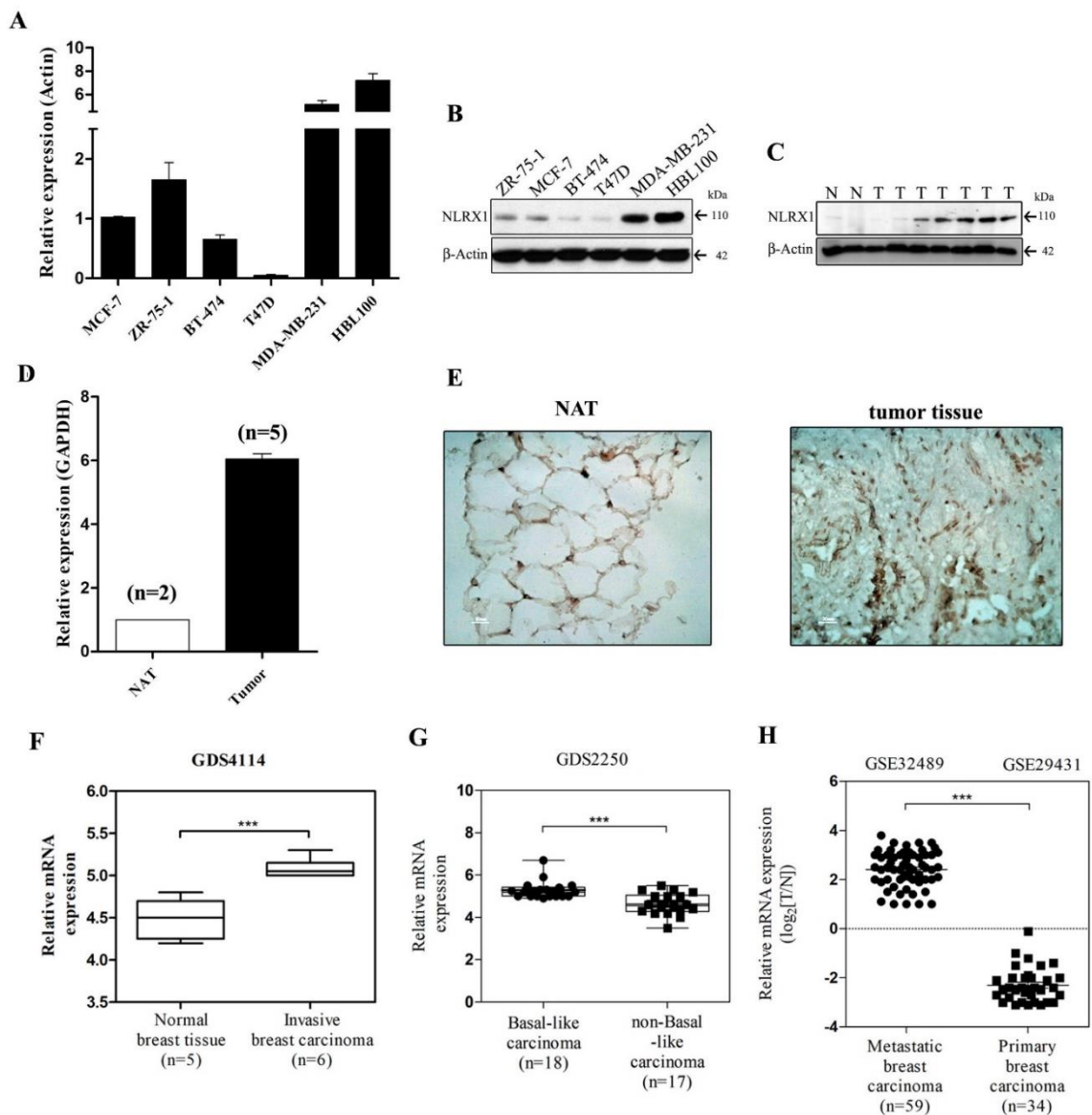
Figure 7.1: Analysis of expression of NLRX1 in breast cancer cell lines and tumor tissues of breast cancer patients. (A) Total RNA was isolated from MCF-7,ZR-75-1, BT-474, T47D, MDA-MB-231 and HBL100 breast cancer cell lines, cDNA prepared and quantitative expression of NLRX1 was analyzed using qPCR. (B) The protein expression level of NLRX1 in same set of breast cancer cell lines was analyzed using immunoblotting against NLRX1. (C) The protein expression level of NLRX1 was analyzed in tumors and non-tumoral adjacent tissue (NAT) using immunoblotting against NLRX1. (D) Total RNA was isolated from tumors and NAT of breast cancer patients and relative expression of NLRX1 was analyzed by qPCR. (E) Immunohistochemical analysis of tumor tissue and NAT was done by incubating the tissue sections with antibody against NLRX1 and detected using DAB staining as described in Materials and method section. Scale bar, 20 mm. (F) NLRX1 gene expression in tissues obtained from Gene Expression Omnibus (GEO) microarray data (GEO accession no. GDS4114). (G) NLRX1 gene expression in breast carcinoma tissues obtained from GEO microarray data (GEO accession no. GDS2250). (H) Breast cancer microarray databases were mined for NLRX1 expression. The raw data were exported from The Cancer Genome Atlas (TCGA) breast cancer database, with the representation of 59 metastatic and 34 primary breast cancer samples. Data is represented as mean ± SEM, Log_2 median-centered ratio expression. Unpaired Mann-Whitney test was used to evaluate the statistical significance. Data in (A) and (D) are representative of three independent experiments, and the results are expressed as mean ± SD. Asterisk (*) denotes significant differences with $p < 0.05$.

7.2 Depletion of NLRX1 represses TNF-α-induced autophagy in breast cancer cells

An elevated autophagy levels contributes to the growth of aggressive tumors by maintaining oxidative metabolism and energy homeostasis in tumor microenvironment (Kimmelman and White, 2017). NLRX1 positively regulates infection-induced autophagy to attenuate the activation of innate immune signaling, however its role in TNF-α-regulated autophagy in cancer cells is not understood. Therefore, we depleted NLRX1 in MDA-MB-231 and HBL100 cells and monitored autophagy levels under different conditions such as in the presence or absence of TNF-α, EBSS (starvation-dependent inducer of autophagy) and Bafilomycin A1 (BafA1, specific V-ATPase inhibitor, used to block lysosomal acidification and degradation). Firstly, we quantified GFP fluorescence intensity in NLRX1-KD MDA-MB-231 cells expressing GFP-LC3 using flow cytometry, a method that has been established for measuring the autophagic flux/turnover (Fig. 7.2A and A'). We observed a significant reduction in total GFP intensity of NLRX1-KD cells in the presence of TNF-α and this reduction in GFP intensity was significantly reversed upon co-

treatment with Baf A1. These results indicated that knockdown of NLRX1 induces autophagy in the presence of TNF-α. To confirm this result, we generated GFP-LC3 stable cell line in HEK293 and monitored the LC3 puncta formation upon NLRX1 knockdown in the presence and absence of TNF-α and Baf A1. Microscopic observation revealed that NLRX1-KD significantly increased GFP-LC3 puncta formation in untreated cells, which further increased significantly in presence of TNF-α as compared to control (Fig. 7.2B, B' and B''). These results confirmed that depletion of NLRX1 induces autophagosome formation, which accumulates in the presence of TNF-α.

To determine whether NLRX1 regulated autophagy in the presence of TNF-α was due to increased autophagosome induction or impaired maturation, we monitored autophagy flux using tandem mCherry–GFP–LC3 reporter assay. GFP fluorescence is quenched in the acidic lysosome while signal from mCherry remains stable, hence double positive, GFP+/mCherry+ puncta corresponds to early autophagosomes whereas only mCherry+ puncta represents mature autolysosomes (Fig. 7.2C). Consistent with the above result, control shRNA cells exhibited an increased number of autolysosomes (mCherry+ puncta) in the presence of TNF-α indicative of an upregulated autophagy flux. The knockdown of NLRX1 increased the number of GFP+/mCherry+ puncta and reduced the number of mCherry positive puncta suggesting an inhibition of TNF-α-induced autophagy flux (Fig. 7.2C'). Treatment with Baf A1 further increased the number of GFP+/mCherry+ puncta in NLRX1-KD cells. We further confirmed this change in autophagy flux by monitoring the turnover of autophagy substrate, p62 (SQSTM1) using tandem mCherry–GFP-p62 reporter assay (Fig. 7.2D'). Similar to LC3, the control cells showed an increased number of mCherry+ puncta whereas NLRX1-KD cells showed a significantly increased number of GFP+/mCherry+ puncta (autophagosomes) in the presence of TNF-α (Fig. 7.2D and E) suggesting that NLRX1 depletion reduces p62 turnover and autophagosome maturation and inhibits TNF-α-induced autophagy flux.

These results were further confirmed by monitoring the turnover of LC3 by immunoblotting. The knockdown of NLRX1 increased basal autophagy levels as compared to control in both MDA-MB-231 and HBL100 cell lines as an increased level of 18 kDa band corresponding to LC3II levels were detected in all treatment conditions (Fig. 7.2F and G).
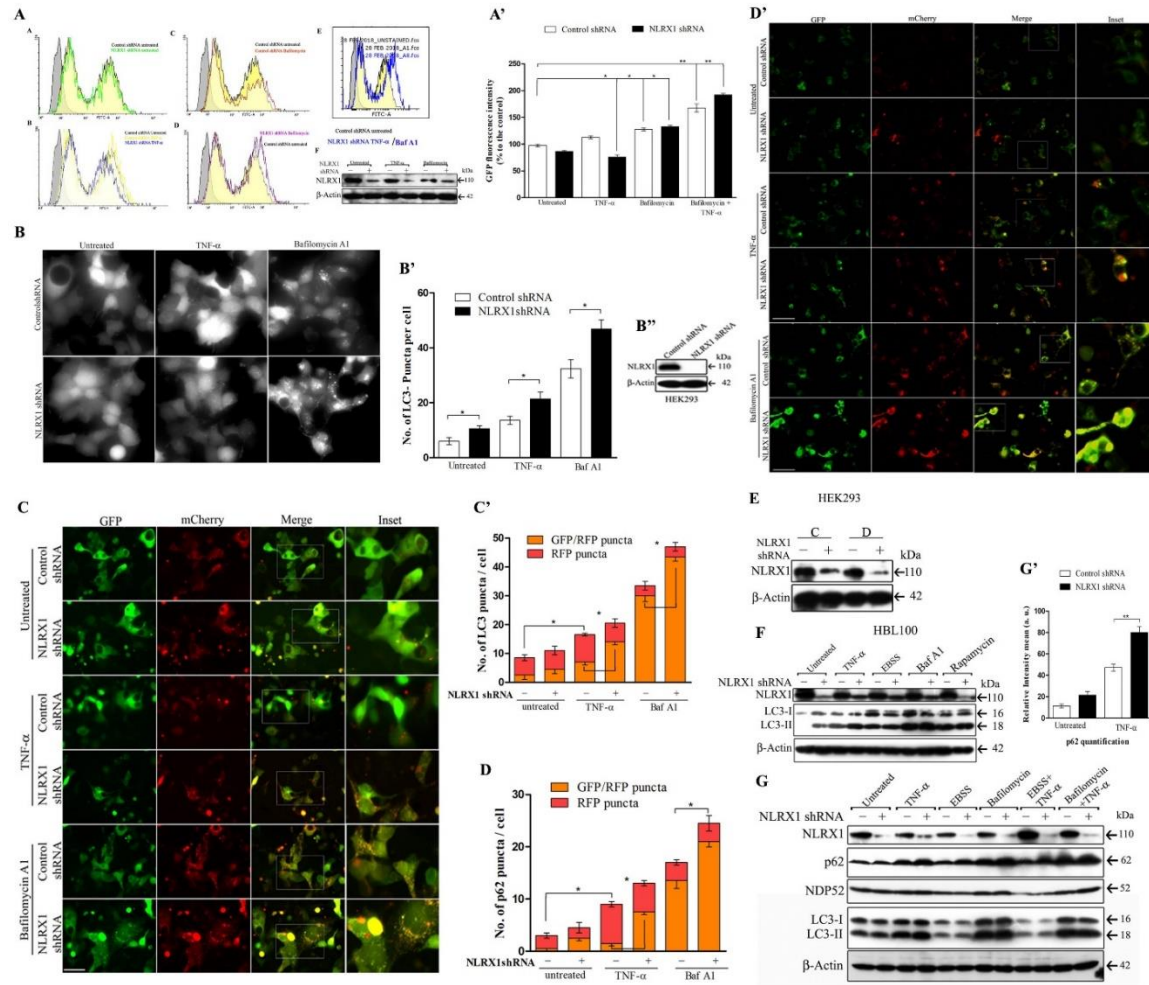
Figure 7.2: Knockdown of NLRX1 leads to accumulation of autophagosomes in the presence of TNF-α in breast cancer cells. (A) and **(A')** MDA-MB-231 cells were co-transfected with control shRNA or NLRX1 shRNA with GFP-LC3 as indicated in method section and treated with TNF-α (10 ng/μl, 24 h), EBSS (4 h) and Baf A1 (100 nM, 8 h). After treatment, cells were collected and total GFP intensity was analyzed by flow cytometry and quantification values were plotted. The confirmation of NLRX1 knockdown in MDA-MB-231 cells by western blotting.**(B)** HEK293-GFP-LC3 stable cells were transfected with control shRNA or NLRX1 shRNA and treated with TNF-α (10 ng/ml, 24 h). After treatments, cells were observed under fluorescent microscope. Scale bar, 20 μm. **(B')** The number of puncta per cell were counted and graph was plotted for numbers of GFP-LC3 puncta per cell. **(B'')** The confirmation of NLRX1 knockdown in HEK293 cells. **(C)**, **(C')**, **(D)** and **(D')** HEK293 cell were co-transfected with control shRNA and NLRX1 shRNA with mCherry-GFP-LC3 or mCherry-GFP-p62 to monitor autophagy flux. After transfection, cells were treated with TNF-α as indicated above and number of GFP+ and mCherry+ puncta formation were observed un-der fluorescent microscope. Quantification of the percentage of GFP+/mCherry+ and only mCherry+ puncta per cell were counted in minimum 100 cells and graph was plotted. **(E)** The confirmation of knock-down of NLRX1 in HEK293 cells of (C) and (D) by western blotting. **(F)** HBL100 cells were transfected

*with control and NLRX1 shRNA. After 48 h of transfection, cells were treated as indicated. After treatment, cell lysates were analyzed by immunoblotting using indicated antibodies. **(G)** MDA-MB-231 cells were transfected with control shRNA or NLRX1 shRNA and treated with TNF-α, EBSS and Baf A1 either alone or in combination as indicated above. After treatment, cells lysates were analyzed by immunoblotting using indicated antibodies.**(G')** The quantification of p62 band intensities in Figure 2F was performed by densitometric analysis using ImageJ v1.45(NIH, MD, USA) software. Data are shown as mean ± SEM (n=3). Asterisk (*) denotes significant differences with p < 0.05.*

The increased level of LC3II was observed in NLRX1-KD MDA-MB-231 cells as compared to control in the presence of TNF-α. Further, cotreatment with BafA1 stabilized both the forms of LC3 (LC3-I/II) and an increased level of LC3II accumulated in NLRX1-KD cells as compared to control cells. Moreover, starvation induced autophagy flux in NLRX1-KD cells remained unchanged relative to control indicating that NLRX1 specifically modulates specifically TNF-α-induced autophagy. Similarly, we examined the expression levels of two known autophagy receptors, p62 and NDP52. Notably, we observed an increased accumulation of p62 in NLRX1-KD cells in the presence of TNF-α which further increased upon co-treatment of Baf A1 as compared to control (Fig. 7.2G and G'). The levels of NDP52 varied marginally in the presence of TNF-α but increased significantly in the presence of TNF-α/Baf A1 in NLRX1-KD cells as compared to control. Altogether, these results confirmed that knockdown of NLRX1 negatively regulates TNF-α- induced autophagy flux in breast cancer cells.

7.3 NLRX1 depletion impairs mitochondrial function in the presence of TNF-α in breast cancer cells

Previous studies reported that the genetic ablation or pharmacological inhibition of mitochondrial respiratory function impaired lysosomal activity leading to accumulation of large lysosomal vacuoles and defective autophagy (Baixauli et al., 2015; Demers-Lamarche et al., 2016). Recent reports from our lab and others have shown that NLRX1 localizes to mitochondria and regulates metabolic function in inflammatory conditions, tissue injury and hepatic steatosis (Kors et al., 2018; Singh et al., 2015; Stokman et al., 2017). We, therefore, hypothesized that loss of NLRX1 in breast cancer cells may alter

mitochondrial function, hence the selective turnover of mitochondria via mitophagy in the presence of TNF-α. To test this hypothesis, we quantified the level of mitochondrial and intracellular ROS in NLRX1-KD MDA-MB-231 cells in the presence TNF-α. The knockdown of NLRX1 showed a significant increase in mitochondrial ROS levels, which further increased in presence of TNF-α (Fig. 7.3A). Treatment of NLRX1-KD cells with Mito-TEMPO (mitochondrial antioxidant) suppressed this NLRX1-dependent ROS accumulation. Similarly, generation of cellular ROS was significantly increased in the NLRX1-KD as compared to control in the presence of TNF-α (Fig. 7.3B). These data indicated that depletion of NLRX1 in breast cancer cells increases TNF-α regulated mitochondrial ROS levels.

Mitochondrial electron transport chain is a major site of ROS generation where individual respiratory chain complexes organizes into supramolecular assemblies called supercomplexes (SC) and regulates electron flux during oxidative stress (Acin-Perez et al., 2008). Hence, we analyzed the relative levels of mitochondrial respiratory chain SCs using BN-PAGE followed by immunoblotting (Fig. 7.3C). Immunodetection of a specific CI protein revealed a decrease in CI-SC in NLRX1-depleted cells in the presence of TNF-α. We also monitored the levels of CIII+CIV-SCs using a complex IV specific antibody which showed decreased levels of CIII+CIV-SCs as well as monomeric CIV in the presence of TNF-α. The levels of SDHA, a CII-specific protein remain unchanged. We further analyzed the activity and assembly of SCs upon NLRX1 silencing in MDA-MB-231 cells in the presence/absence of TNF-α by in-gel activity staining (Fig. 7.3D). In-gel assay for CI and CIV revealed a prominent staining for CI present in CI+CIII+CIV-SCs in control and NLRX1-KD cells whereas activity decreased significantly in NLRX1-KD cells in the presence of TNF-α indicating a loss of NADH dehydrogenase activity in all bands corresponding to supercomplexes of CI (Fig. 7.3D'). In contrast, knockdown of NLRX1 alone significantly decreased the cytochrome c oxidase activity in CIII+CIV-SCs which further reduced in the presence of TNF-α. We observed a marked decrease in cytochrome c oxidase activity of monomeric CIV upon NLRX1 knockdown cell the presence of TNF-α. These observations were further confirmed by enzyme kinetic study of NADH-dependent electron transfer from CI to CIII and CIV enzyme activity in the presence of TNF-α (Fig. 7.3E). We observed a significant decrease in NADH reduction in NLRX1-KD cells in
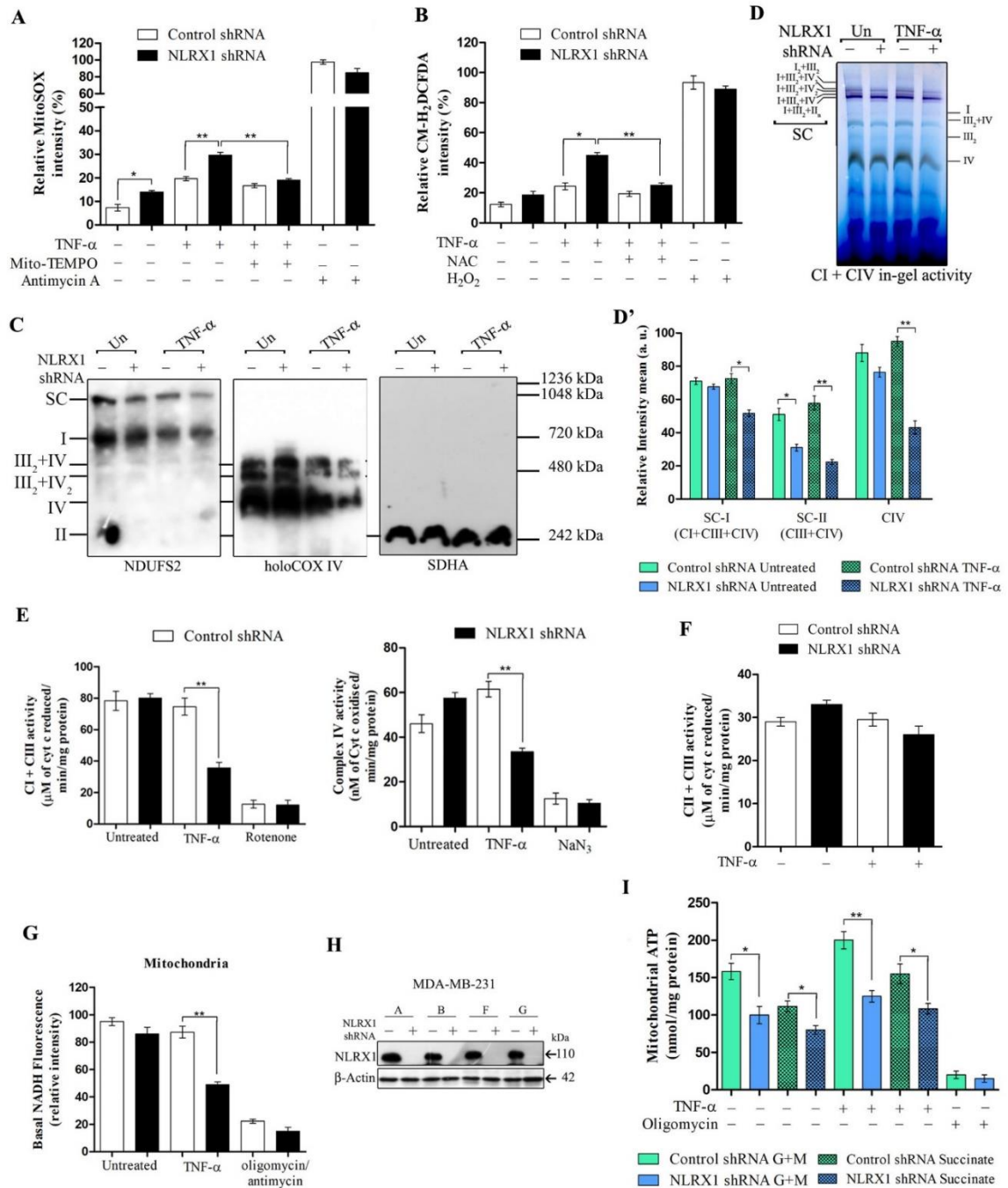
Figure 7.3: NLRX1 knockdown alters TNF-α-regulated mitochondrial bioenergetic capacity in breast cancer cells. (A) and (B) MDA-MB-231 cells were transfected with control shRNA or NLRX1 shRNA and treated with TNF-α (10 ng/ml), antimycin A (10 μg/ml), NAC (5 mM), H₂O₂ (50 μM) and Mito-Tempo (10 μM) either alone or in combination for 24 h. After treatment, mitochondrial ROS levels and intracellular ROS levels were quantified as indicated in method section. (C) MDA-MB-231 cells were transfected with control shRNA or NLRX1 shRNA and treated with TNF-α as indicated above. After treatment, the levels of CI, CIII and CIV-containing supercomplexes as well as individual complexes were analyzed by BN-PAGE

*followed by immunoblotting with indicated antibodies (**D**) or in-gel activity staining specific for CI and CIV as described in method section. (**D'**) The quantification of band intensities in (D) detected by in-gel staining was performed by densitometric analysis using ImageJ v1.45(NIH, MD, USA) software. (**E**) and (**F**) MDA-MB-231 cells were transfected with control shRNA and NLRX1 shRNA and treated with TNF-α, rotenone (100 nM) and NaN$_3$ (20 mM) for 24 h either alone or in combination. After treatment, the enzyme activities of CI to CIII, CIV and CII + CIII enzyme activity electron transport were quantified from cell lysates using a spectrophotometer. (**G**) MDA-MB-231 cells were transfected with control shRNA and NLRX1 shRNA and treated with TNF-α and oligomycin/antimycin (5 μM/4 μM) for 24 h. After treatment, mitochondria were isolated and NADH levels were quantified as described in method section. (**H**) The confirmation of NLRX1 knockdown in MDA-MB-231 cells of (A), (B), (G) and (H) by western blotting. (**I**) MDA-MB-231 cells were transfected and treated as indicated above. After treatment, mitochondria were isolated and mitochondrial ATP synthesis were measured by kinetic luminescence assay as described in method section. Data are shown as mean ± SEM (n=3). Asterisk (*) denotes significant differences with p < 0.05.*

presence of TNF-α suggesting inhibition of electron transport from CI to CIII. Similar to in-gel activity, the spectrophotometric assay showed decreased CIV activity in NLRX1-KD cells in the presence of TNF-α (Fig. 7.3E').   In contrast, the activity of FADH$_2$-dependent electron transfer from CII to CIII remain unchanged (Fig. 7.3F). These data prompted us to analyze the mitochondrial NADH levels in NLRX1-depleted cells. The NADH levels decreased significantly in NLRX1-KD cells in the presence of TNF-α as compared to control (Fig. 7.3G and H). Consequently, NLRX1-KD cells showed reduced mitochondrial ATP synthesis both in the presence or absence of TNF-α as compared to control cells (Fig. 7.3I). The results here strongly suggested that NLRX1 silencing impairs TNF-α-regulated mitochondrial respiratory function resulting in decreased mitochondrial ATP synthesis and NAD$^+$/NADH imbalance in breast cancer cells.
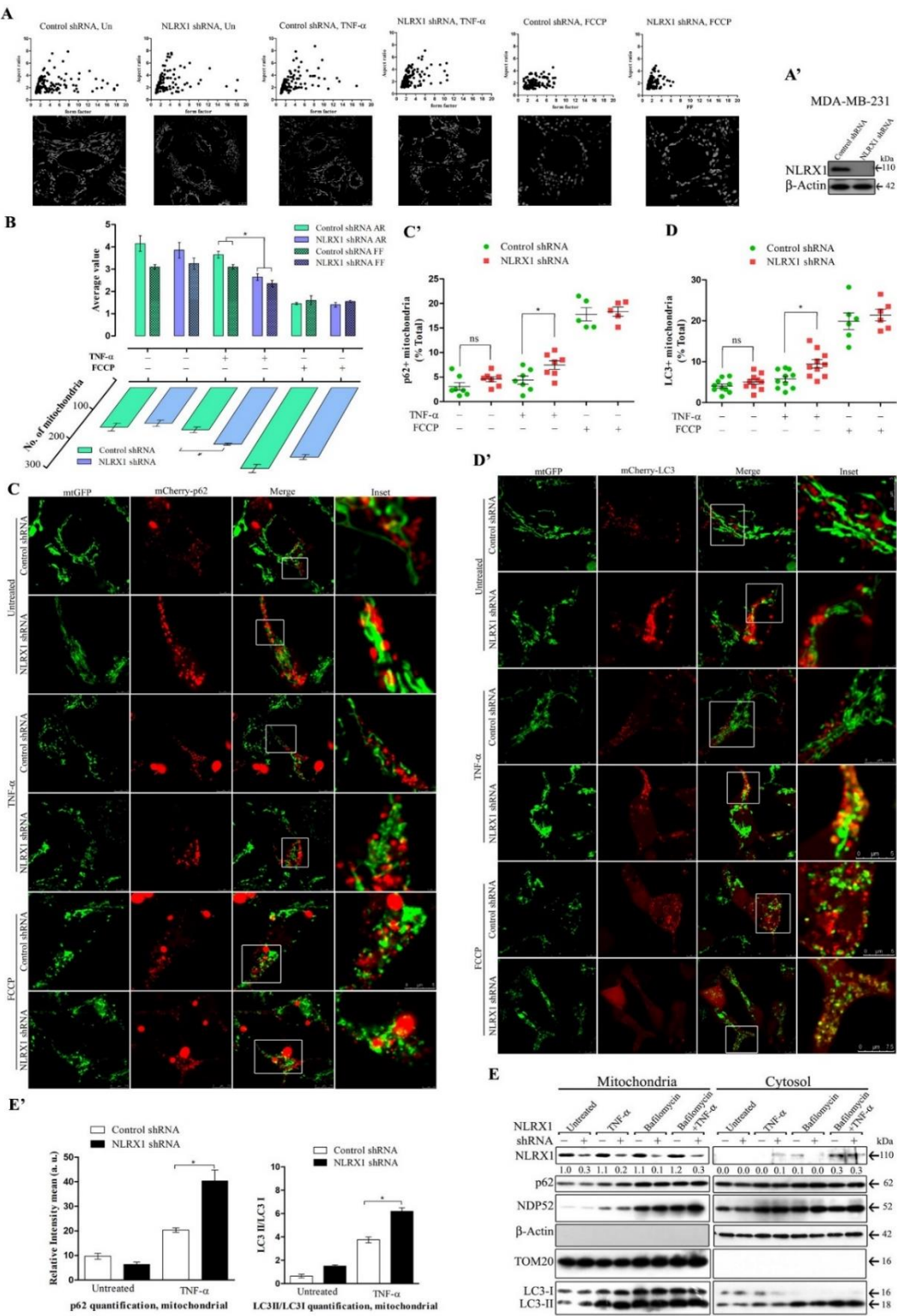
7.4 NLRX1 silencing alters mitochondrial dynamics and inhibits TNF-α-induced mitophagy in breast cancer cells

Dysregulation of mitochondrial function causes alteration of fission/fusion dynamics leading to increased fragmentation of mitochondrial network. The selective elimination of damaged mitochondria through mitophagy is essential for the maintenance of physio-

logical ROS levels and bioenergetic homeostasis (Mishra and Chan, 2016). The compromised mitochondria functions observed in NLRX1-depleted breast cancer cells suggested a possible alteration in mitochondrial dynamics and mitophagy. To confirm this, we monitored the mitochondrial morphology in the presence of TNF-α by TMRM staining, a cell-permeant cationic fluorescent dye, which accumulates in mitochondria (Fig. 7.4A). Normal tubular and interconnected mitochondrial population were observed in untreated control and NLRX1-KD MDA-MB-231 cells whereas number of punctuated mitochondria increased in NLRX1-KD cells in presence of TNF-α (Fig. 7.4A and A'). We further analyzed mitochondrial morphologies using a morphometric tool that calculate aspect ratio (AR) and form factor (FF). Both parameters have a minimal value of 1, which represents a perfect circle, and the value increases as mitochondria elongate. Mitochondria from NLRX1-depleted cells had lower values of FF and AR in the presence of TNF-α compared to control cells (Fig. 7.4B). This indicated mitochondrial fragmentation in NLRX1-KD cells in presence of TNF-α. As a positive control, cells were treated with FCCP, a protonophore, which causes dissipation of mitochondrial transmembrane potential (ΔΨm). FCCP treatment increased mitochondrial fragmentation in both control and NLRX1-KD cells. These results showed that depletion of NLRX1 induces fragmentation of mitochondrial network in the presence of TNF-α.

Autophagy receptor proteins p62 and NDP52 recognizes damaged mitochondria and promotes their autophagic clearance through LC3II-dependent recruitment to the phagophore (Baumann, 2015). Hence, we analyzed the recruitment of mCherry-p62 and mCherry-LC3 to mitochondria using mtGFP-HEK293 stable cells using live-cell confocal imaging. We observed discrete mCherry-p62 puncta in control cells, which further increased in NLRX1 knockdown cells but its association with mitochondria did not alter significantly (Fig. 7.4C). However, NLRX1-KD cells treated with TNF-α showed p62-puncta, which significantly colocalized with mitochondria (Fig. 7.4C'). This observation was further confirmed in the presence of FCCP (as a positive control), which showed fragmented mitochondria colocalizing with mCherry-p62 in both control and NLRX1-KD cells. Similarly, the colocalization of mCherry-LC3 with mitochondria was analyzed (Fig. 7.4D'). The cells expressing mCherry-LC3 and transfected with control shRNA showed diffuse cytoplasmic distribution in the absence of TNF-α whereas knockdown of

NLRX1 alone induced mCherry positive LC3 puncta representing newly formed autoph-
agosome/autolysosomes. However, the colocalization of LC3 puncta with mitochondria

Figure 7.4: NLRX1 knockdown alters mitochondrial dynamics and represses TNF-α-regulated mitoph-agy flux in breast cancer cells. (A) and (A'') MDA-MB-231 cells were transfected with control shRNA and NLRX1 shRNA and treated with TNF-α (10 ng/ml) for 24 h. After treatment, cells were stained with 100 nM TMRM and analysis of mitochondrial morphology by form factor and aspect ratio were quantified as de-scribed in method section. Scale bar, 10µm. The graph plotted for form factor and aspect ratio of individu-al mitochondria from the representative image are shown. The confirmation of knockdown of NLRX1 in MDA-MB-231 cells by western blotting. (B) Average values of form factor and aspect ratio, as well as number of mitochondria, from five confocal images for each experimental set are plotted. (C), (C'), (D) and (D') mtGFP-HEK293 cells were co-transfected with control shRNA or NLRX1 shRNA and mCherry-p62 or mCherry-LC3 as described in method section. After transfection, cells were treated with TNF-α (10 ng/ml) for 24 h. After treatment live cell imaging was performed to visualize the colocalization of mCherry-p62 or mCherry-LC3 with GFP signal of mitochondria. The quantification of colocalization signal was performed as described in method section and the graph plot-ted. Scale bar, 5µm. (E) MDA-MB-231 cells were transfected with control shRNA and NLRX1 shRNA and treated with TNF-α or Baf A1 either alone or in combination as indicated above. After treatment, mitochondria and cytosolic fraction were isolated and immunoblotted with indicated antibodies. (E') Densitometric analysis of mitochondrial p62 levels and LC3II/LC3-I ratio in (E)

did not alter significantly. In contrast, NLRX1-depleted cells exhibited an increased colo-calization of mitochondria with mCherrypositiveLC3 puncta in the presence of TNF-α as compared to control (Fig. 7.4D). As a positive control, FCCP treatment induced mito-chondrial fragmentation and increased its colocalization with LC3 in both control and NLRX1-KD cells.

To further confirm these observations, we isolated mitochondrial and cytosolic fraction from control and NLRX1-depleted MDA-MB-231 cells in the presence or absence of TNF-α and/or BafA1 and analyzed the levels of p62/NDP52 and LC3 by immunoblotting (Fig. 7.4E). We observed a band of 110 kDa corresponding to NLRX1 in mitochondrial fraction. The level of cytosolic-p62 did not altered significantly between control and NLRX1-KD cells in the presence of TNF-α and/or BafA1. In contrast, lower levels of p62 were detected in mitochondrial fraction of control and NLRX1-KD cells which in-creased significantly in NLRX1-depleted cells in presence of TNF-α and further accu-mulated upon co-treatment with Baf A1 as compared to control cells (Fig. 7.4E'). Similar to p62, an increased level of NDP52 was observed in the mitochondrial fraction of

NLRX1-depleted cells in the presence of TNF-α and/or Baf A1whereas the cytosolic levels remain unchanged. The analysis of LC3 levels revealed an increased level of 18kDa band corresponding to conjugated LC3II in mitochondrial fraction of NLRX1-KD cells both in the presence of TNF-α and/or Baf A1. In agreement with the microscopic observation, these results confirmed that depletion of NLRX1 leads to translocation of p62/NDP52-autophagy receptors, on damaged mitochondria and subsequently recruit LC3II for the formation of mitophagosome in presence of TNF-α.

7.5 Depletion of NLRX1 causes abnormal accumulation of lysosomal vacuoles and increases lysosomal biogenesis in the presence of TNF-α.

Increased accumulation of p62/LC3II levels in NLRX1 depleted cells suggested that turnover of mitochondria by mitophagy is inhibited due to impaired maturation of autophagosomes to autolysosomes. To confirm this, we examined the morphology of lysosomes and its activity in presence of TNF-α. First, we analyzed the cross talk of mitochondria with lysosomal compartments in a mCherry-LAMP1 HEK293 stable cell line under a confocal microscope (Fig. 7.5A). We observed a relatively large number of LAMP1+ lysosomes in NLRX1-KD cells, which is agreement with above finding that depletion of NLRX1 in breast cancer cells increases basal autophagy. However, the association of mCherry-LAMP1 with mitochondria was not altered as compared to control. Treatment of NLRX1-KD cells with TNF-α showed a significant increase in colocalization of LAMP1+ lysosomes with mitochondria (Fig. 7.5B and C). We also observed large lysosomal vesicles containing GFP+ mitochondria suggesting an increased mitophagy in these cells. Treatment with FCCP and Baf A1 further induced mitophagy and lead to an increased accumulation of large LAMP1+vesicles containing damaged mitochondria as observed in NLRX1-KD cells in the presence of TNF-α. We further examined the lysosomal morphology and calculated their relative population in control and NLRX1-KD cells from same experiment. LAMP1-positive lysosomes were binned into three categories according to their diameter: normal lysosomes (< 1.0 µm), intermediate lysosomes (1.0-2.5 µm) and LAMP1 vacuoles (> 3.0 µm). As defined, both control and NLRX1-KD showed normal population of LAMP1+ lysosomes whereas the population of intermedi-

ate lysosomes in NLRX1-KD cells significantly increased in presence of TNF-α as compared to control (Fig. 7.5D). In addition to intermediate lysosomes, the number of LAMP1+ vacuoles increased in both control and NLRX1-KD cells in the presence of FCCP and Baf A1. These results suggested that knockdown of NLRX1 increases mitophagy flux but results in accumulation of large lysosomal vesicles containing damaged mitochondria in the presence of TNF-α.

During lysosomal stress, nuclear translocation of cytosolic TFEB activates a transcriptional program of coordinated lysosomal expression and regulation (CLEAR) network to increase autophagy and lysosomal biogenesis and function (Settembre et al., 2013). An increased accumulation of abnormal LAMP1 +vesicles in NLRX1-KD cells in the presence of TNF-α, may trigger lysosomal biogenesis as rescue mechanism, hence, we analyzed the TNF-α regulated nuclear translocation of TFEB in control and NLRX1-KD MDA-MB-231 cells. Confocal analysis showed a significant increase in nuclear translocation of TFEB-GFP in NLRX1-depleted cells in the presence of TNF-α (Fig. 7.5E, F and G). This observation was further confirmed by subcellular fractionation and immunoblotting using anti-TFEB antibody. An increased level of TFEB was observed in nuclear fraction of NLRX1-KD MDA-MB-231 cells in the presence of TNF-α (Fig. 7.5H) which further accumulated upon co-treatment with lysosomal stress inducer, Baf A1.

We also monitored the transcriptional activation of TFEB target genes of lysosomal function to further confirm the lysosomal biogenesis. The knockdown of NLRX1 in MDA-MB-231 cells resulted in an increased expression of genes involved in lysosomal function (ATP6V0D1) and biogenesis (LAPTM4A and LAMP1) in the presence of TNF-α (Fig. 7.5I and J). These evidences suggested that depletion of NLRX1 results in accumulation of abnormal lysosomal compartments which is associated with transcriptional activation of TFEB responsive genes of lysosome biogenesis in the presence of TNF-α in breast cancer cells
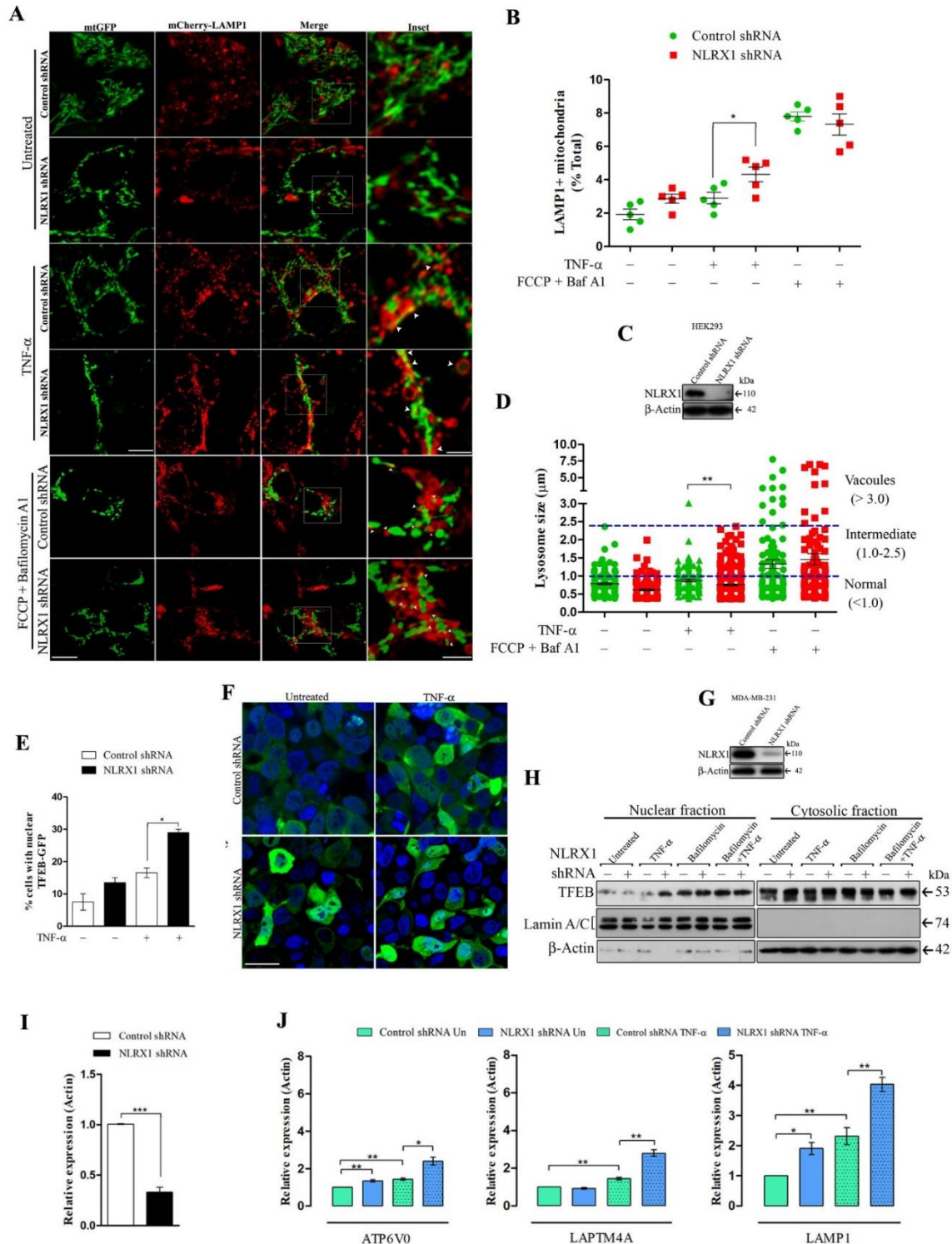
Figure 7.5: NLRX1 depletion initiates nuclear translocation of TFEB to induce lysosomal biogenesis in the presence of TNF-α. (A) *mCherry-LAMP1 HEK293 stable cell line were co-transfected with mtGFP and control shRNA or NLRX1 shRNA and treated with TNF-α.After treatment, live cell imaging was performed to visualize the colocalization of mCherry-LAMP1 with GFP signal of mitochondria as described in*

*method section. Scale bar, 10 μm.(**B**) The quantification of colocalization signal from (A) was performed as described in method section and the graph plotted. (**C**) The confirmation of knockdown of NLRX1 in HEK293 .(**D**) The size distribution of lysosomes from experimental sets in (A) was analyzed using ImageJ and plotted as described in method section. (**E**) and (**F**) MDA-MB-231 cells were co-transfected with TFEB-GFP and control shRNA or NLRX1 shRNA and treated with TNF-α for 24 h. The cells were fixed and counterstained with DAPI and monitored under confocal microscope and number of cells with nuclear TFEB-GFP were counted and plotted as described in method section. (**G**) The confirmation of knockdown of NLRX1 in MDA-MB-231 cells.(**H**) MDA-MB-231 cells were transfected with control shRNA or NLRX1 shRNA and treated with TNF-α and Baf A1 either alone or in combination. After treatment, nuclear and cytosolic fraction were isolated and analyzed by immunoblotting using indicated antibodies. (**I**) and (**J**) MDA-MB-231 cells were transfected with control shRNA or NLRX1 shRNA and treated with TNF-α. After treatment, total RNA was extracted, cDNA was prepared and relative expression levels of NLRX1, ATP6V0D1, LAPTM4A and LAMP1were quantified using qPCR. Data are representative of three independent experiments, and the results are expressed as mean ± SD. Asterisk (*) denotes significant differences with $p < 0.05$.*

7.6 NLRX1-regulated mitochondrial function modulates lysosomal activity in the presence of TNF-α in breast cancer cells

To characterize the functional status of TFEB-induced increase in lysosomal population, we assessed lysosomal acidification in NLRX1-KD cells with a specific lysosomal pH-sensitive probe by FACS in the presence and absence of TNF-α (Fig. 7.6A). Lysosensor signal significantly decreased in NLRX1-KD cells as compared to control in the presence of TNF-α indicating defective lysosomal acidification (Fig. 7.6B). We measured the activity of lysosomal protease cathepsin B and acid lipase in these cells (Fig. 7.6C and D). Consistent with reduced lysosomal acidification observed in NLRX1-KD cells, cathepsin B and lysosomal acid lipase activity significantly decreased in NLRX1-KD cells in the presence of TNF-α. Similarly, acid phosphatase activity significantly decreased in NLRX1-KD cells in the presence of TNF-α (Fig. 7.6E). These findings suggested that NLRX1 knockdown leads to lysosomal dysfunction in presence of TNF-α. Further, transcriptional activation of lysosomal biogenesis through TFEB was unable to maintain lysosomal function and autophagy flux in NLRX1-depleted cells in the presence of TNF-α.
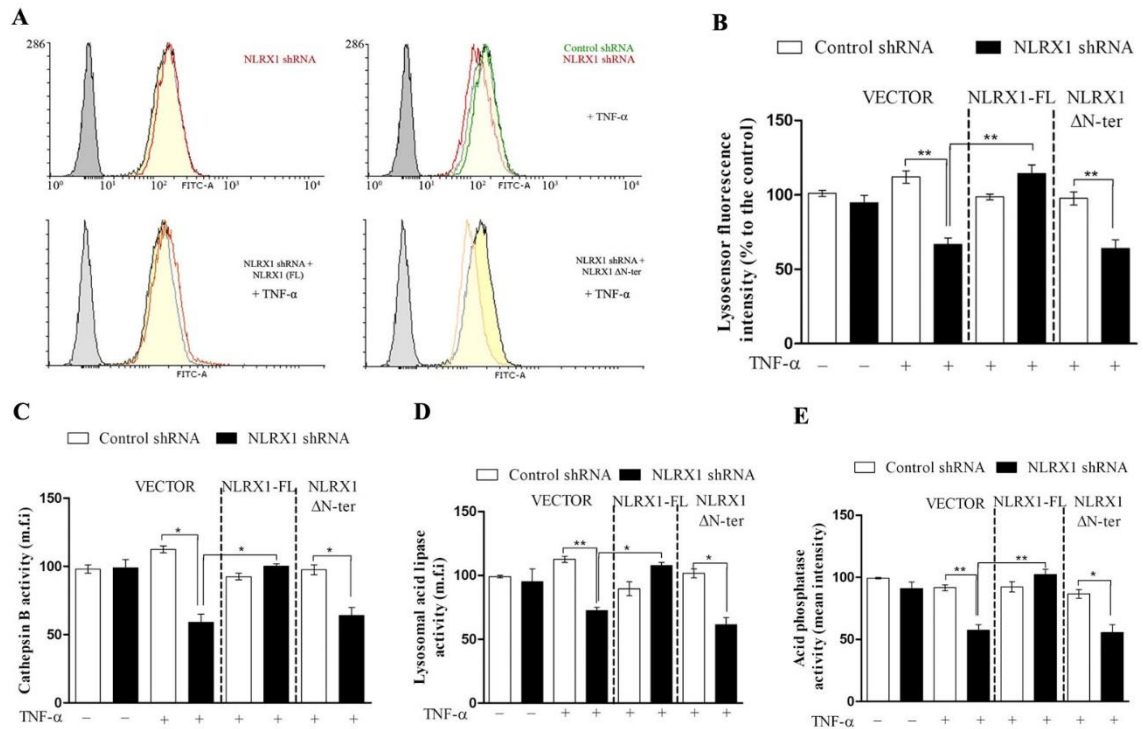
Figure 7.6: NLRX1 regulates lysosomal function in the presence of TNF-α in breast cancer cells *. (A) and (B) Control shRNA and NLRX1 shRNA MDA-MB-231 cells were co-transfected with vector, NLRX1-full length and NRX1 ΔN-ter constructs and treated with TNF-α for 24 h. After treatment, cells were stained with Lysosensor™ Green as described in method section and fluorescence intensity was measured by flow cytometry and quantification values were plotted. (C) and (D) MDA-MB-231 cells were transfected and treated as in (A). After treatment, Cathepsin B activity (C) and acid lipase activity (D) was analyzed by fluorescence assay as described in method section. (E) MDA-MB-231 cells were transfected as indicated in (A) and treated with TNF-α. After treatment, acid phosphatase activity was determined by quantification of color intensity of acid phosphatase substrate present in the cell lysate as described in method section. Data are representative of three independent experiments, and the results are expressed as mean ± SEM. Asterisk (*) denotes significant differences with p < 0.05.*

Recent reports have demonstrated that loss of mitochondrial function disrupts lysosomal structure and its activity, thus providing a direct link between maintenance of mitochondrial homeostasis and lysosomal degradation capacity (Baixauli et al., 2015; Demers-Lamarche et al., 2016). Therefore, we asked if restoring mitochondrial function could rescue lysosomal function in NLRX1-depleted cells in the presence of TNF-α. To answer this, we over-expressed full length NLRX1 and N-terminal deletion mutant (NLRX1 ΔN-ter,) lacking mitochondria localization signal in NLRX1-KD MDA-MB-231 cells and analyzed the functional status of lysosomal compartment in the presence and absence of

TNF-α. Interestingly, we detected an enhanced acidification of lysosomes (reduced pH) by FACS in the NLRX1-KD cells co-transfected with full length NLRX1 but not with NLRX1ΔN-ter in the presence of TNF-α (Fig. 7.6A and B). Similarly, ectopic expression of full length NLRX1 but not NLRX1-ΔN-ter completely restored the cathepsin B, acid lipase and acid phosphatase activity in NLRX1-depleted breast cancer cells in the presence of TNF-α (Fig. 6C, D and E). These experiments suggest that mitochondrial localization of NLRX1 is essential for rescuing defective lysosome functions in NLRX1 KD MDA-MB-231 cells. Altogether, these results strongly suggested that depletion of NLRX1 in breast cancer cells altered mitochondrial form and function leading to abnormal, non-functional lysosomes in the presence of TNF-α

7.7 Loss of NLRX1 inhibits OxPhos-dependent cell proliferation, clonogenic ability and migration of breast cancer cells

We monitored the changes in growth rates of the NLRX1-KD MDA-MB-231 cells in a medium containing alternative nutrient carbon sources, namely glucose or galactose (Fig. 7A). In high-glucose medium the growth rate of the control and NLRX1-KD cells showed no significant change, up to day five in absence of TNF-α. In contrast, the growth rate of NLRX1-KD cells decreased significantly at the end of the fifth day as compared to control in the presence of TNF-α (Fig. 7B and B'). The overall growth rate of both control and NLRX1-KD cells in galactose-containing medium was lower, as compared to the high glucose medium. The growth rate of the NLRX1-KD cells decreased both in the presence and absence of TNF-α in galactose medium. NLRX1-KD cells demonstrated an unchanged proliferation rate during the initial 48 h, thereafter rate gradually declined and showed diminished proliferation after day 5 suggesting that decreased proliferation rate of NLRX1 KD cells due to compromised OxPhos activity.

We further monitored the clonogenic ability of HBL100 and MDA-MB-231 cells upon NLRX1 silencing in the presence and absence of TNF-α. Consistent with the proliferation rate, number of colony forming units significantly decreased in NLRX1-depleted
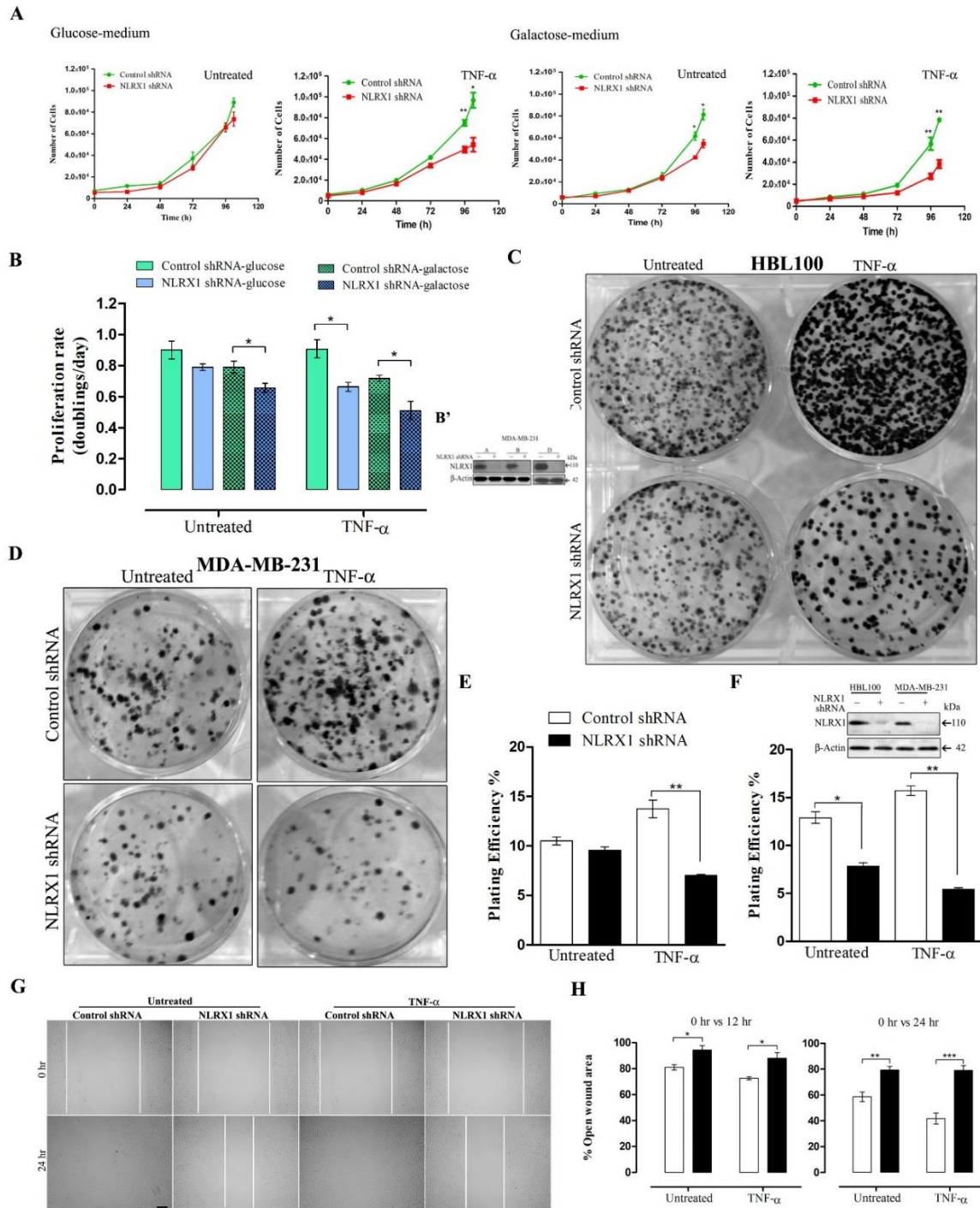
Figure 7.7: *NLRX1 regulates mitochondrial respiration-dependent cell proliferation, clonogenic ability and migration of breast cancer cells in the presence of TNF-α. (A) MDA-MB-231 cells were transfected with control shRNA or NLRX1 shRNA, seeded in galactose-containing medium in the presence of TNF-α. Growth curves were determined by cell count normalized to cell number at t = 0 when media conditions were applied, were assessed for five consecutive days and used to calculate proliferation rate. (B) Prolifer-*

*ation rates of the cells in respective medium were determined as described in method section. (**B'**) The confirmation of knockdown of NLRX1 in MDA-MB-231 cells. (**C**), (**D**), (**E**) and (**F**) MDA-MB-231 and HBL100 cells were transfected with control shRNA or NLRX1 shRNA and treated with TNF-α. After treatment, clonogenic activity was assessed by counting number of colony forming units and plotted as plating efficiency as described in method section. The knockdown of NLRX1 in both cell lines was confirmed by western blotting. (**G**) and (**H**) MDA-MB-231 cells were transfected and treated as in (C) and cell migration was analyzed by scratch assay after 12 h and later at 24 h as described in method section. Scale bar, 20 µm. Data are representative of three independent experiments, and the results are expressed as mean ± SEM. Asterisk (*) denotes significant differences with p < 0.05.*

HBL100 cells in the presence of TNF-α also shown as plating efficiency (Fig. 7C and D). The knockdown of NLRX1 alone decreased the clonogenic ability of MDA-MB-231 cells while it further reduced in the presence of TNF-α (Fig. 7E and F). Similarly, we monitored the migration ability of NLRX1-KD breast cancer cells in the presence and absence of TNF-α using scratch assay. We observed a significant increase in open wound area of NLRX1-KD cells both at 12 h in the presence and absence of TNF-α, which further increased at 24 h, which decreased significantly at both 12 h and 24 h in the presence of TNF-α (Fig. 7G and H). These data clearly suggested that NLRX1-regulated mitochondrial function play a critical role in regulating the clonogenic ability, proliferation and migration ability of breast cancer cells.

7.8 Discussion

NLRX1 expression is differentially regulated in multiple human cancer subtypes suggesting a complex role of NLRX1 in regulation of pathways associated with tumorigenesis (Coutermarsh-Ott et al., 2016; Hu et al., 2018; Lei and Maloy, 2016). We found that NLRX1 expression is significantly down regulated in human breast cancer cell lines with low metastasis potential while it was upregulated in aggressive triple negative breast cancer cell lines as well as in tumor tissues of breast cancer patients. These observations suggested a tumor suppressive role of NLRX1 in primary solid tumors of breast and colorectal cancer as previously reported (Lei and Maloy, 2016; Singh et al., 2015). The upregulated expression of NLRX1 reflects a high invasiveness potential and a higher tendency towards tumor relapse or metastasis as observed in the clinical data (Coutermarsh-

Ott et al., 2016). Aggressive breast tumors have a high prevalence of activating mutations in oncogene(s) leading to poor prognosis in patients and exhibit an increased dependency on autophagy for survival in an inflammatory microenvironment (McCarthy, 2011).

The recent reports from the study of tumor immune microenvironment suggest that metastatic cancer cells acquire amplification or loss of genes involved in innate immune signaling to adapt the complex tumor microenvironment (Bakhoum and Cantley, 2018). These proteins localize to mitochondria and its contact site probably to integrate inflammation, bioenergetics and metabolism. The recent studies reporting the functional link between mitochondrial metabolism and lysosomal activity prompted us to investigate the role of NLRX1 in regulation of autophagy in presence of TNF-α, which is one of the predominant cytokine in tumor microenvironment (Baixauli et al., 2015; Demers-Lamarche et al., 2016; Lippitz, 2013). Quantitative and microscopic analysis of autophagy levels in NLRX1-KD breast cancer cells showed an increased number of autophagosome formation in presence of TNF-α. Interestingly, autophagy flux experiment and immunoblotting revealed an impaired maturation of LC3-containing autophagosomes and accumulation of p62/NDP52 in NLRX1-depleted cells in presence of TNF-α. These results suggested that NLRX1 is essential for maintaining TNF-α-regulated autophagy flux in breast cancer cells. NLRX1 regulated autophagy flux and its implication is not limited in breast cancer cells and has also been observed in metastatic head and neck squamous cell carcinoma (HNSCC) (Lei et al., 2016), hence, this should be further investigated in cancer models from different origin.

The emerging reports suggest that mitochondrial function is essential for the lysosomal function and hence the maintenance of autophagy flux (Baixauli et al., 2015). The analysis of mitochondrial functions in presence of TNF-α strongly suggests that NLRX1 regulates the activity and organization of mitochondrial respiratory chain complexes and their active supercomplexes. This further strengthens our hypothesis of NLRX1 role in maintenance of mitochondrial OxPhos function along with reports from other groups (Kors et al., 2018; Stokman et al., 2017). Consequently, NLRX1 KD cells showed reduced mitochondrial ATP generation and increased levels of TNF-α-induced ROS accumulation while steady-state ATP levels remained unchanged. The analysis of mitochon-

drial morphology in NLRX1-depleted breast cancer cell lines showed altered mitochondrial dynamics and increased mitochondrial fragmentation in the presence of TNF-α. Interestingly, confocal microscopy showed increased level of p62/NDP52 autophagy receptors on mitochondria suggesting the accumulation of mitochondria-containing autophagosomes in NLRX1 KD breast cancer cells in presence of TNF-α. The observations in the current study is further supported by findings from *Stokman et al* demonstrating that loss of NLRX1 resulted in an increased population of fragmented mitochondrial network usually present in lysosomal-vacuole like structure during renal ischemia-reperfusion injury (Stokman et al., 2017).

The defective autophagic clearance results from either non-functional lysosomes or inhibition of lysosomal biogenesis (Lim and Zoncu, 2016). Indeed, we observed an increased accumulation of enlarged lysosomal compartment associated with mitochondria in NLRX1-depleted cell in presence of TNF-α. The alteration in lysosomal acidification and function in NLRX1-depleted cells further suggested the induction of lysosomal stress in these cells in presence of TNF-α. TFEB is localized on lysosome in complex with mTORC1 and translocates to nucleus during lysosomal stress to induce lysosomal biogenesis (Sardiello et al., 2009). The defective autophagy observed in NLRX1-depleted cells showed an increased nuclear localization of TFEB in presence of TNF-α, suggesting the activation of TFEB pathway as a cellular response to rescue lysosomal stress. TFEB regulates the CLEAR network of genes involved in lysosomal and autophagy pathway. The restoration of lysosomal function in NLRX1-depleted cells through ectopic expression of NLRX1 strongly supports the role of NLRX1-regulated mitochondrial metabolism in the regulation of lysosomal function. These findings further support the hypothesis that lysosomal activity is functionally coupled to maintenance of a functional mitochondrial metabolic state in cell. Emerging evidences suggest that mitochondrial dysfunction and downstream oxidative stress play an important role in regulating lysosomal activity to maintain cellular homeostasis. This has important implication in regulating immunomodulatory function of T cell and etiology of neurodegenerative diseases (Baixauli et al., 2015; Demers-Lamarche et al., 2016). However, the role of NLRX1 in these patho-physiological conditions still needs to be investigated.

We recently reported that NLRX1 regulates the levels of mature mitochondrial transcripts and hence the activity and organization of OxPhos complex in under normal conditions (Singh et al., 2018). Therefore, NLRX1 may alter mitochondrial ROS and ATP generation through the same mechanism in presence of TNF-α. The evidences presented here further support our hypothesis that NLRX1 modulates the assembly and activity of mitochondrial electron transport chain complexes in presence of TNF-α. This further contributes to the reprogramming of metabolic pathways of tumor cells by altering the balance of NAD+/NADH and promoting aerobic glycolysis (Sullivan et al., 2015). In addition to mitochondrial metabolism, metastatic tumors show increased dependence on autophagy for normal growth (Guo and White, 2016). Indeed, we observed a diminished proliferation rate of NLRX1-deficient breast cancer cells in an OxPhos medium containing only galactose whereas proliferation rate remain unchanged in glycolytic medium containing only glucose in the presence of TNF-α. Previously, we and others, reported that NLRX1 acts as a tumor suppressor as its expression was downregulated in ER/PR positive breast cancer cells as well as in colon carcinoma (Lei and Maloy, 2016; Singh et al., 2015). Similarly, it was observed that stimulation with TNF-α resulted in exacerbated proliferation and expression of the intestinal stem cell marker in intestinal organoids lacking NLRX1 (Tattoli et al., 2016). The emerging evidences suggest that persistent selection pressure during the course of primary tumor formation results in acquisition of specific genes and associated pathway providing survival advantage for further growth and metastasis (Bakhoum and Cantley, 2018). NLRX1 is highly expressed in ER/PR negative breast cancer cells. Similarly, STING , an upstream innate immune regulator which acts as tumor suppressor, is upregulated in metastatic breast cancer cells. A previous study demonstrated the crosstalk between STING and NLRX1 innate immune signaling through direct interaction during viral infection (Mar and Schoggins, 2016). Hence, the regulation STING/NLRX1 pathway may provide survival advantage by limiting inflammatory response and cell death and enhancing autophagy flux in metastatic cancer cells. An increased dependency of metastatic tumors on autophagy have led to the therapeutic intervention by using drugs such as hydroxychloroquine (HCQ), which interferes with lysosome function at the terminal step of autophagic degradation in clinical trials (White and DiPaola, 2009). Our observation that NLRX1-regulated mitochondrial function de-

creases clonogenic and migration ability of breast cancer cells by modulating TNF-α-induced autophagy provide a functional link between mitochondrial metabolism and autophagy, which could further allow the designing of novel therapeutic strategies aimed at controlling human breast tumorigenesis.

In conclusion, we provided evidences that NLRX1 is an essential mitochondrial protein of metastatic breast cancer cells, which is required to preserve the mitochondrial homeostasis by regulating lysosomal function in the presence of TNF-α. This in turn is important in maintaining tumorigenic activity of breast cancer cells. The absence of NLRX1 in benign tumors, as well as ER/PR positive breast cancer cells suggest its tumor suppressor role as reported previously (Singh et al., 2015). An increased expression of NLRX1 in metastatic breast tumors and triple negative breast cancer cells may regulate mitochondrial metabolic function and its turnover through mitophagy. Thus, NLRX1 may support the tumorigenic potential of aggressive breast cancer cells by maintaining energy homeostasis and preserving organelle function. This is another example of tumor cell adaptive response where levels of innate immune sensors are regulated in a cell autonomous manner to provide survival advantage within tumor microenvironment (Xia et al., 2016).